

Analytical Expression for RMS DC Link Capacitor Current in a Three-Level Inverter

K. S. Gopalakrishnan, Soumitra Das
 Department of Electrical Engineering
 Indian Institute of Science
 Bangalore, India
 ashwinkrishnan121@ee.iisc.ernet.in
 soumitradas@ee.iisc.ernet.in

G. Narayanan
 Department of Electrical Engineering
 Indian Institute of Science
 Bangalore, India
 gnar@ee.iisc.ernet.in

Abstract— An analytical expression is derived for calculating the rms current through the DC link capacitor in a three level inverter. The output current of the inverter is assumed to sinusoidal. Variations in the capacitor rms current with modulation index as well as line side power factor are studied. The worst case current stress on the capacitor is determined. This is required for sizing the capacitor and is useful for predicting the capacitor losses and life. The analytical expression derived is validated through simulations and experimental results at a number of operating points.

Index Terms—Three-level inverter, Multi level inverter, DC link capacitor, capacitor current ripple, duty ratio.

I. INTRODUCTION

THREE level inverters are increasingly used in high power drive applications since these have more number of switches in series and can withstand higher voltage levels. These inverters also offer better quality voltage waveform with less harmonic content than two-level inverters as has been shown in [1].

The DC link capacitor is an important component in a three-level inverter. Selection of appropriate DC link capacitor is a critical step in the design of a three-level inverter [2]. The rms value of the current which might flow through the capacitor has to be predicted so that capacitors of appropriate rms current ratings could be chosen. Also the operating voltage and especially the working temperature have a significant influence on the working life of the electrolytic capacitor [3]. Therefore the working temperature of the capacitor needs to be predicted. This depends on the rms current flowing through the capacitor as shown in (1).

$$T_c = T_a + I_{CAPRMS}^2 R_{ESR} R_{th,c-a} \quad (1)$$

Where, T_c is the working temperature of capacitor; T_a is the ambient temperature; R_{ESR} denotes the equivalent series resistance of the capacitor; $R_{th,c-a}$ is the thermal resistance between capacitor can and ambient.

The methods for calculating RMS ripple current in literature

usually rely on spectral analysis and digital simulations. It is convenient to have an analytical expression for the rms capacitor current in terms of the operating conditions of the inverter. The operating condition can be defined by modulation depth and the power factor angle of the inverter output current.

An analytical expression has been derived for the capacitor RMS current for a two level converter in [4], [5]. In this paper, a similar expression is derived for the RMS current through the DC link capacitor in a three-level inverter. The RMS current is expressed in terms of modulation index (M), power factor angle (ϕ) and the amplitude of the output current (I_N). Now the knowledge of the influence of the operating conditions on the capacitor current RMS value can easily be used to determine the worst case current stress.

II. ANALYTICAL EXPRESSION FOR RMS CURRENT

A. Duty Ratio:

A three-phase three-level neutral-point clamped (NPC) inverter is shown in Fig. 1. The switches are controlled by sine-triangle modulation scheme [6]. In a three-level inverter leg, switch SX1 ($X=R, Y, B$) and SX3 switch in a complementary fashion, while SX2 and SX4 are complementary. The duty ratio of the four switches in R-phase leg of a three-level inverter can be expressed in terms of modulation index M and fundamental angle ' θ ' as given below.

$$\begin{aligned} d_{SR1} &= M \sin(\theta) && \text{when } \sin(\theta) > 0 \\ &= 0 && \text{when } \sin(\theta) < 0 \\ d_{SR2} &= 1 && \text{when } \sin(\theta) > 0 \\ &= 1 + M \sin(\theta) && \text{when } \sin(\theta) < 0 \\ d_{SR3} &= 1 - M \sin(\theta) && \text{when } \sin(\theta) > 0 \\ &= 1 && \text{when } \sin(\theta) < 0 \end{aligned} \quad (2)$$

$$d_{SR4} = 0 \quad \text{when } \sin(\theta) > 0$$

$$= -M \sin(\theta) \quad \text{when } \sin(\theta) < 0$$

The expressions for the duty ratio are similar for the switches in other two legs (except for the phase shift). The variations of the duty ratios of the switches SR1, SY1, SB1 over a line cycle are plotted in Fig. 2.

B. Average and rms DC link current:

The output currents of the converter are considered to be pure sinusoids without any harmonic components as defined in (3), where ' ϕ ' is the angle by which the phase current lags behind the phase voltage.

$$i_R = I_N \sin(\theta - \phi)$$

$$i_Y = I_N \sin\left(\theta - \phi - \frac{2\pi}{3}\right) \quad (3)$$

$$i_B = I_N \sin\left(\theta - \phi - \frac{4\pi}{3}\right)$$

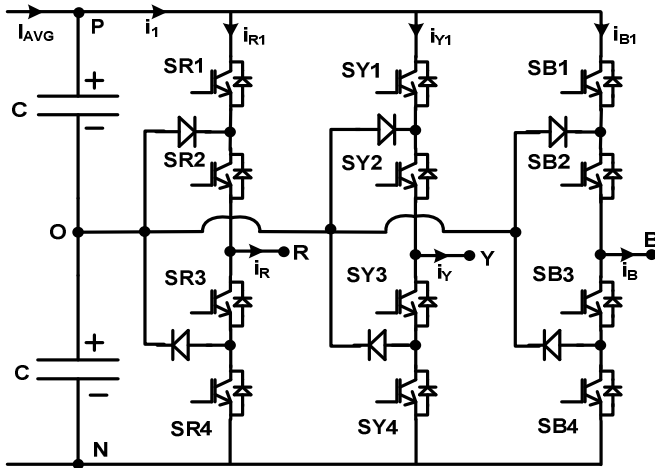


Fig. 1: A three-level neutral-point clamped converter

As seen from Fig. 1, the current through the top device in a leg (say, SR1) depends on the output current of the leg (say, i_R) and the switching functions of top two devices in the leg (say, S_{SR1} and S_{SR2}) as shown in (4). The switching function of a switch is defined as 1, when the switch is 'ON'; otherwise it is equal to 0.

$$i_{R1} = S_{SR1} * S_{SR2} * i_R$$

$$i_{Y1} = S_{SY1} * S_{SY2} * i_Y \quad (4)$$

$$i_{B1} = S_{SB1} * S_{SB2} * i_B$$

The DC link current (i_l) can be expressed in terms of the currents through switch SR1, SY1 and SB1 as shown in (5).

$$i_l = i_{R1} + i_{Y1} + i_{B1} \quad (5)$$

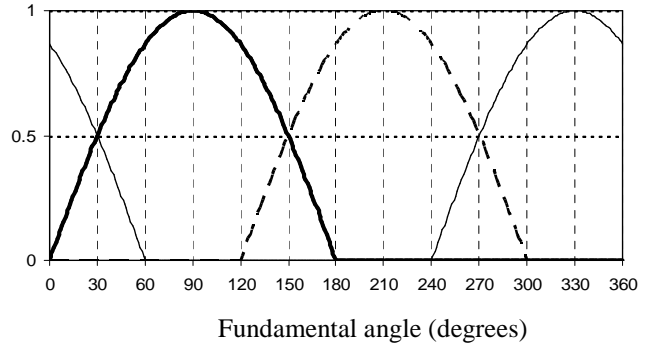


Fig. 2: Plot of duty ratios of switches SR1, SY1, SB1

As seen from the Fig. 2, the duty ratio plots have three-phase symmetry. Hence, it is enough to calculate the average and rms values of the DC link current over a 120° duration. The 120° interval considered here is between 90° and 210° shown in Fig. 2. Calculations in the four sub-intervals within this interval are explained below.

a. Sub-interval 1: $90^\circ < \theta < 120^\circ$

In the first sub-interval, $90^\circ < \theta < 120^\circ$, the duty ratios of switches SY1 and SB1 are zero as seen from Fig. 2. The switches SY1 and SB1 are 'OFF' in this duration, and the switches SY3 and SB3 are 'ON'; there would not be any current through the anti-parallel diodes of SY1 and SB1. Hence, the current i_l is equal to i_{R1} . The average DC link current within a carrier cycle, $i_{l,avg}(\theta)$ is given by (6), and the average input DC link current in this 30° interval can be expressed in terms of $i_{l,avg}(\theta)$ as shown in (7).

$$i_{l,avg}(\theta) = i_R * d_{SR1} \quad (6)$$

$$I_{AVG1} = \frac{6}{\pi} \int_{\frac{\pi}{2}}^{\frac{3\pi}{2}} i_{l,avg}(\theta) d\theta \quad (7)$$

Similarly, the rms DC link current in a switching cycle and the rms input DC link current over this 30° interval are given by (8) and (9) respectively.

$$i_{1,RMS}^2(\theta) = i_R^2 * d_{SR1} \quad (8)$$

$$I_{RMS1} = \sqrt{\frac{6}{\pi} \int_{\frac{\pi}{2}}^{\frac{3\pi}{2}} i_{1,RMS}^2(\theta) d\theta} \quad (9)$$

b. Sub-interval 2: $120^\circ < \theta < 150^\circ$

In this interval, the duty ratio of switch SR1 (d_{SR1}) is greater than the duty ratio of switch SY1 (d_{SY1}); the duty ratio of SB1

(d_{SB1}) is 0 as seen from Fig. 2. The three-phase duty ratios in a particular carrier cycle within this interval are reproduced in Fig. 3. In the first carrier half-cycle, during time T_0 , all the switches (SR1, SY1 and SB1) are 'OFF' as shown in Fig. 3; only switch SR1 is 'ON' during T_1 , while both SR1 and SY1 are 'ON' during T_2 . The time intervals can be expressed in terms of duty ratios as follows.

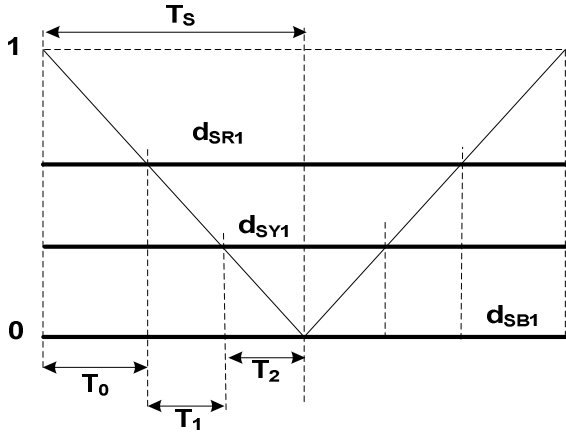


Fig. 3: The plot of duty ratios of switches SR1, SY1, SB1 during a particular switching window in $120^\circ < \theta < 150^\circ$.

$$\begin{aligned} T_1 &= (d_{SR1} - d_{SY1}) * T_s \\ T_2 &= d_{SY1} * T_s \\ T_0 &= T_s - (T_1 + T_2) \end{aligned} \quad (10)$$

It is clear that i_{R1} flows during T_1 ; during the interval T_2 , i_{R1} and i_{Y1} flow; i_{B1} is zero during the whole sub-cycle. The expression for average DC link current over the sub-cycle is given by (11).

$$\begin{aligned} i_{1,avg}(\theta) &= \frac{1}{T_s} [i_R T_1 + (i_R + i_Y) T_2] \\ &= \frac{1}{T_s} [i_R T_1 - i_B T_2] \\ &= i_R (d_{SR1} - d_{SY1}) - i_B d_{SY1} \end{aligned} \quad (11)$$

The average DC link current over the 30° interval is given by (12).

$$I_{AVG2} = \frac{6}{\pi} \int_{\frac{2\pi}{3}}^{\frac{5\pi}{6}} i_{1,avg}(\theta) d\theta \quad (12)$$

The RMS value of DC link current over the sub-cycle and RMS DC link current over the 30° interval are defined in (13) and (14), respectively

$$i_{1,RMS}^2(\theta) = (i_R^2 * (d_{SR1} - d_{SY1})) + (i_B^2 * d_{SY1}) \quad (13)$$

$$I_{RMS2} = \sqrt{\frac{6}{\pi} \int_{\frac{2\pi}{3}}^{\frac{5\pi}{6}} i_{1,RMS}^2(\theta) d\theta} \quad (14)$$

c. Sub-interval 3: $150^\circ < \theta < 180^\circ$

In the interval, d_{SY1} is greater than d_{SR1} , while d_{SB1} is 0. Hence, the expressions for average DC link current for any sub-cycle in this interval and average input DC link current over the 30° interval are also given in (15) and (16), respectively.

$$i_{1,avg}(\theta) = (i_Y * (d_{SY1} - d_{SR1})) - (i_B * d_{SR1}) \quad (15)$$

$$I_{AVG3} = \frac{6}{\pi} \int_{\frac{5\pi}{6}}^{\pi} i_{1,avg}(\theta) d\theta \quad (16)$$

The RMS DC link current over a sub-cycle in this interval and RMS DC link current over the 30° interval are defined below.

$$i_{1,RMS}^2(\theta) = (i_Y^2 * (d_{SY1} - d_{SR1})) + (i_B^2 * d_{SR1}) \quad (17)$$

$$I_{RMS3} = \sqrt{\frac{6}{\pi} \int_{\frac{5\pi}{6}}^{\pi} i_{1,RMS}^2(\theta) d\theta} \quad (18)$$

d. Sub-interval 4: $180^\circ < \theta < 210^\circ$

In this interval, the Duty-Ratios of switches SR1 and SB1 are 0. Therefore i_{B1} and i_{R1} are 0 and $i_l = i_{Y1}$. Hence, the expressions for average DC link current for any sub-cycle in this interval and average input DC link current over the 30° interval are given by (19) and (20), respectively.

$$i_{1,avg}(\theta) = i_Y * d_{SY1} \quad (19)$$

$$I_{AVG4} = \frac{6}{\pi} \int_{\pi}^{\frac{7\pi}{6}} i_{1,avg}(\theta) d\theta \quad (20)$$

The RMS DC link current over a sub-cycle and the RMS DC link current over the 30° interval are expressed in (21) and (22), respectively.

$$i_{1,RMS}^2(\theta) = i_Y^2 * d_{SY1} \quad (21)$$

$$I_{RMS4} = \sqrt{\frac{6}{\pi} \int_{\pi}^{\frac{7\pi}{6}} i_{1,RMS}^2(\theta) d\theta} \quad (22)$$

The overall average DC link current is given below.

$$\begin{aligned} I_{AVG} &= \frac{I_{AVG1} + I_{AVG2} + I_{AVG3} + I_{AVG4}}{4} \\ &= \frac{3}{4} I_N M \cos(\phi) \end{aligned} \quad (23)$$

The overall RMS DC link current is defined in (24)

$$I_{RMS} = \sqrt{\frac{I_{RMS1}^2 + I_{RMS2}^2 + I_{RMS3}^2 + I_{RMS4}^2}{4}} = \sqrt{\frac{3I_N^2 * M * ((\sqrt{3} + (\cos(2\phi) * (\frac{2}{\sqrt{3}}))))}{4\pi}} \quad (24)$$

C. RMS Current in capacitor DC link

The capacitor RMS current can be expressed mathematically as shown below.

$$I_{CAPRMS} = \sqrt{I_{RMS}^2 - I_{AVG}^2} = \sqrt{\frac{3I_N^2 M^2}{4\pi} \left(\sqrt{3} + \cos(2\phi) \left(\frac{2}{\sqrt{3}} \right) \right) - \frac{9}{16} (I_N M)^2 \cos^2(\phi)} \quad (25)$$

It is seen in the equation (25) that the capacitor ripple current is a function of both modulation index (M) and the power factor of load current (ϕ).

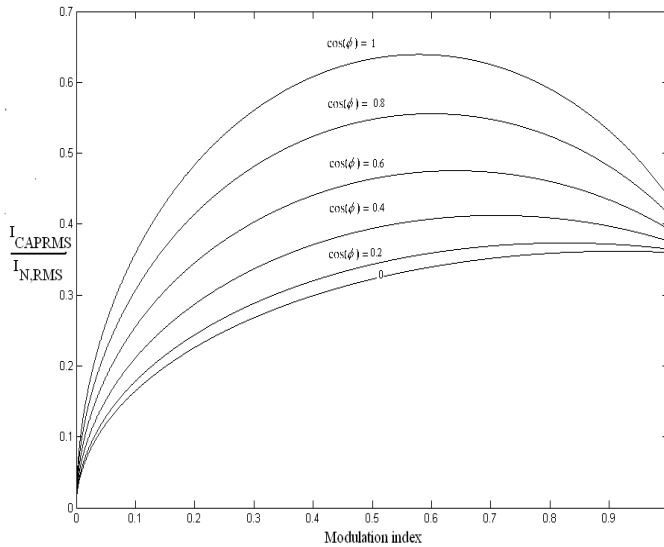


Fig. 4 Variation in capacitor ripple current with modulation index for different power-factor angles of the load.

The partial differentiation of the mean square value of the capacitor current is done with respect to power factor angle (ϕ), keeping M constant, to find the operating power factor for maximum ripple current, as given in (26). It is seen that the ripple current is maximum at unity power factor load ($\phi=0$).

$$\frac{\delta I_{CAPRMS}^2}{\delta \phi} = I_N^2 \left(0 + \frac{\cos(\phi) * \sqrt{3} * M * (-\sin(\phi))}{2\pi} \right) = 0 \quad (26)$$

Now to find operating modulation index, where the

capacitor ripple current is maximum for a unity power factor load, the mean square capacitor current is differentiated partially with respect to M as shown in (27). It is found that the DC link capacitor ripple current is highest at a modulation index (M) of 0.612.

$$\frac{\delta I_{CAPRMS}^2}{\delta M} = I_N^2 \left(\frac{\sqrt{3}}{\pi} + \frac{\cos^2(\phi) * \sqrt{3} * M}{4\pi} - \frac{9 * M^2}{16} \right) = 0 \quad (27)$$

The capacitor ripple current is plotted for varying modulation indices at different power factor angle as shown in Fig. 5. For a 50 kVA, 415 V three-phase three-level inverter, the worst case RMS DC link capacitor current stress is found to be 45 A with a rated load current of 70 A.

III. SIMULATION RESULTS

Simulation is carried out in MATLAB SIMULINK platform for a 50 kVA, 415V three-level converter. The maximum load current is taken as 98 A. As mentioned earlier the load current of the three-level inverter is considered to be a pure sine wave of 98A amplitude. Sine-triangle pulse-width modulation technique is used to find the switching functions of all the switches. The current through the top switch of each leg is found using (4). These currents through all the three legs are added together to get the DC link current. The DC link current is then subtracted from the average current from the source side to obtain the capacitor current. The plot of load current (i_R), switching function (S_{SR1}), the input current to top switches of all three legs (i_{R1} , i_{Y1} , i_{B1}), the DC link current (i_j) and the capacitor current (i_{CAP}) are shown in Fig. 5 for unity power factor load and modulation index of 0.61.

The modulation index and power factor angle of the load current are varied; the corresponding RMS values of DC link capacitor current are found using simulation. Table I indicates the analytical and simulated values of RMS DC link capacitor current corresponding to various conditions. It is seen from Table I that the analytical values and simulated values are matching reasonably well.

IV. EXPERIMENTAL VERIFICATION

An IGBT-based three-level inverter is switched using sine triangle PWM at a carrier frequency of 1.5 kHz. The DC bus is charged to 300 V, and the load is an R-L load. The experimental set up is shown in Fig-6.

The measured load current and capacitor current for a modulation index of 0.6 and power factor angle of 0.707 is shown in fig 7. The measurements are carried out at three different modulation indexes, namely 0.4, 0.6 and 0.8 and at three different power factors, ie 0.242(lag), 0.707(lag) and 1. The analytical and measured values of average DC link current and the rms capacitor current are tabulated in Table II.

Table I: Analytical and simulated values of the rms DC link capacitor current

M	Φ (degree)	Analytical Value (Amp)	Simulation Value (Amp)
0.2	0	33.28	33.285
0.4	0	42.22	44.23
0.6	0	45.01	45.015
0.8	0	42.86	42.87
1	0	34.87	34.91
0.6	30 (lag)	41.45	42.43
0.6	60 (lag)	33.2	36.14
0.6	90 (lag)	28.18	32.60
0.6	90 (lead)	28.18	32.60
0.6	120(lag)	33.2	33.21
0.6	180(lag)	45	45

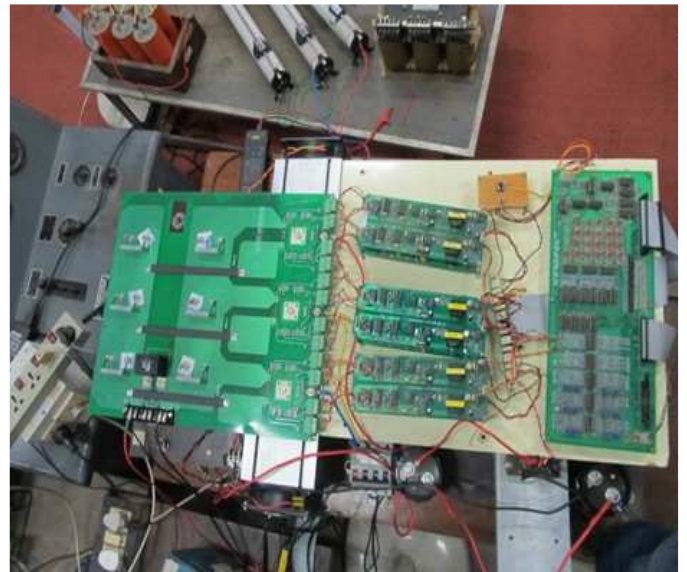


Fig. 6 The experimental set up

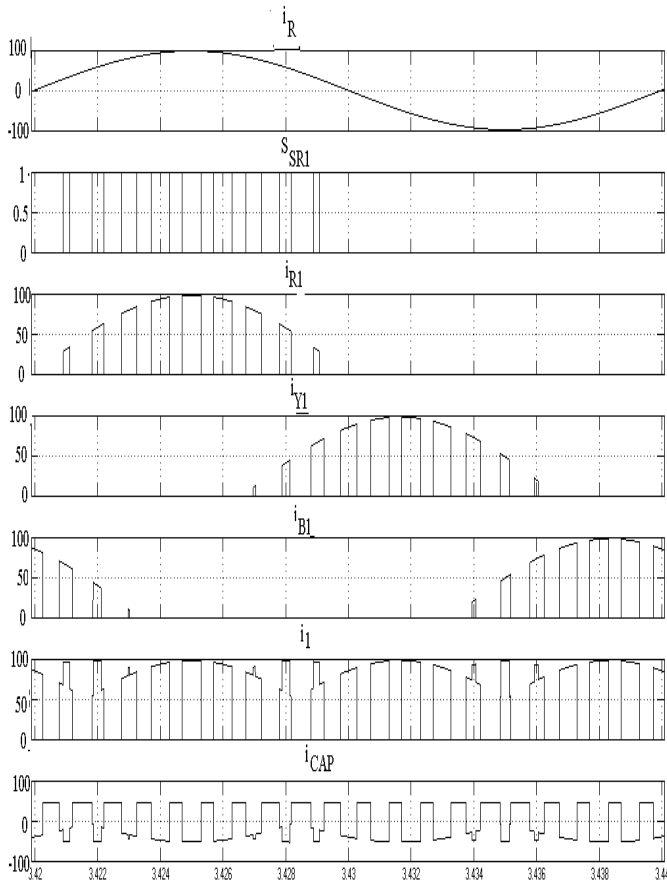


Fig. 5 The load current, switching function of switch SR1, input current to all the legs, DC link current and the capacitor current for a modulation index of 0.61 and unity power factor load current.

As can be seen from the table the analytical and measured values closely match with each other. The deviation at unity power factor load is because the load current no longer remains sinusoidal as has been assumed in the derivation.

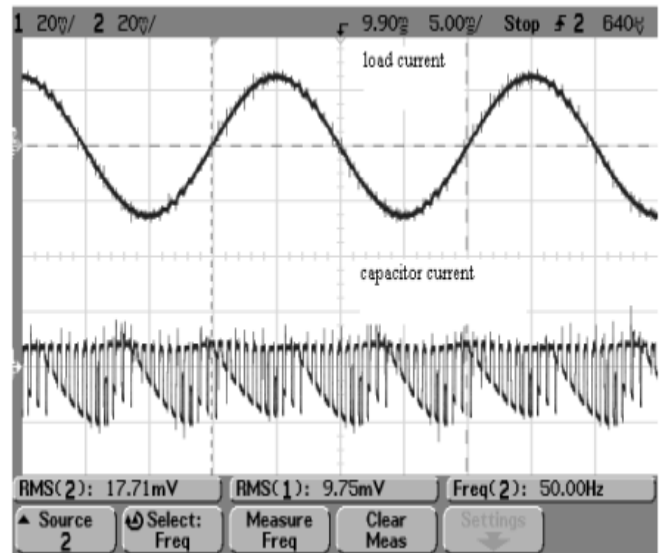


Fig. 7 Measured load current and capacitor current for a modulation index of 0.6 and power factor of 0.707

Table II: Analytical and measured values of I_{AVG} and I_{CAPRMS}

Power factor	M	I_N (Amp)	Analytical values		Measured Values	
			I_{AVG} (Amp)	I_{CAPRMS} (Amp)	I_{AVG} (Amp)	I_{CAPRMS} (Amp)
0.707	0.8	3.5	1.48	1.359	1.435	1.341
0.707	0.6	2.5	0.795	0.958	0.821	0.975
0.707	0.4	1.67	0.354	0.579	0.383	0.585
0.242	0.8	4.815	0.699	1.632	0.678	1.554
0.242	0.6	3.587	0.39	1.077	0.404	1.032
0.242	0.4	2.393	0.174	0.599	0.203	0.553
1	0.8	3.73	2.238	1.631	2.37	1.653
1	0.6	3.73	1.679	1.713	1.895	1.805
1	0.4	3.73	1.125	1.615	1.491	2

V. CONCLUSION

In this paper, an analytical expression for calculating the current stress on a DC link capacitor of a three level, three phase inverter is derived. The analytical expression is

validated through simulations and experiments. The experimental and analytical values agree reasonably well.

REFERENCES

- [1] A. Nabae, I. Takahashi, and H. Akagi, "A new neutral-point-clamped PWM inverter," IEEE Trans. Ind. Appl., vol. IA-17, no. 5, pp. 518–523, Sep./Oct. 1981.
- [2] C. Newton, M. Sumner and T. Alexander, "The investigation and development of a multi level voltage source inverter", Proc 6th Conference on Power Electronics and Variable Speed Drives, pp. 317-321, Sept 1996.
- [3] R. P. McManus, "The effects of operating parameters on aluminium electrolytic capacitor reliability in switched mode converters," Proc. 6th National Solid-State Power Conversion Conf., pp. 13.1-13.5, 1979.
- [4] J.W. Kolar and S.D. Round, "Analytical calculation of the rms current stress on the DC-link capacitor of voltage-PWM converter system" in IEE Proc. Electric Power Applications, vol.153, no.4, pp.535-543 July 2006.
- [5] P.D. Evans and R.J. Hill-cottingham, "DC link current in PWM inverters" in IEE Proc. Electric Power Applications, vol. 133, no.4, pp.217-224 July 1986.
- [6] R. K. Behera, T. V. Dixit and S. P. Das, "Analysis of experimental investigation of various carrier-based modulation schemes for three level neutral point clamped inverter-fed induction motor drive," International Conference on Power Electronics, Drives and Energy Systems (PEDES '06, New Delhi Dec. 2006.